*Seventh International Conference on CFD in the Minerals and Process Industries*
*CSIRO, Melbourne, Australia*
*9-11 December 2009*

# INTERFACE-TURBULENCE INTERACTIONS AND BUBBLE DYNAMICS

**Petar LIOVIC[1*], Djamel LAKEHAL[2]**

[1] CSIRO Materials Science and Engineering, Highett, Victoria 3190, AUSTRALIA
[2] ASCOMP GmbH, Zurich, SWITZERLAND
*Corresponding author, E-mail address: Petar.Liovic@csiro.au

## ABSTRACT

A methodology and numerical schemes for the Large Eddy and Interface Simulation (LEIS) of interfacial flows is introduced. A procedure for unresolved surface tension closure is also presented that involves filtering at coarser length scales to determine the existence and magnitude of sub-grid scale curvature. The unresolved surface tension closure is combined with high-order schemes for super-grid spatial discretisation of the Navier-Stokes equations and proper capturing of interface turbulence asymptotic behaviour. The unresolved surface tension model can act to smooth spatial curvature variations and dampens parasitic modes, and can alternatively restore subgrid-scale interface wrinkling when super-grid scale resolution underpredicts local curvature. The unresolved curvature modelling is validated on a problem with non-uniform curvature variation, and its utility is demonstrated in the bubble-bursting interfacial flow problem.

## NOMENCLATURE

| | |
|---|---|
| $t$ | time |
| $\mathbf{x}$ | position vector for spatial coordinate $(x, y, z)$ |
| $\mathbf{u}$ | velocity |
| $P$ | pressure |
| $S$ | fluid species |
| $C$ | fractional volume phase indicator (color) |
| $\rho$ | density |
| $\mu$ | dynamic viscosity |
| $\Pi$ | Cauchy stress (pressure + viscous forces) |
| $\mathbf{g}$ | acceleration due to gravity |
| $\sigma$ | surface tension |
| $\kappa$ | interfacial curvature |
| $\hat{\mathbf{n}}$ | unit interface normal |
| $\delta$ | interfacial delta function |
| $Re$ | Reynolds number |
| $\tau_N$ | normal-to-interface component of viscous stress |
| $\tau_S$ | shear-to-interface component of viscous stress |
| $f$ | dependent variable to be filtered |
| $\tau^{SGS}$ | sub-grid scale stress tensor |
| $\varepsilon_C$ | commutation error closure term |
| $\varepsilon_d$ | sub-grid scale inter-phase net force closure term |
| $\varepsilon_\sigma$ | unresolved surface tension closure term |
| $h$ | (interface) height function |
| $\delta V$ | volume of mesh cell ( $= \delta x_i \delta y_j \delta z_k$ ) |

## INTRODUCTION

The concept of surface wrinkling is rather well established in the field of combustion, in the context of very small flame surface deformation due to turbulence. In gas-liquid flows such as bubble rise, drop impact and wave breaking, deformations of gas-liquid interfaces are also interface wrinkling, but have traditionally been referred to using alternative terminologies. Interfacial instabilities that introduce higher-wavenumber modes into the interface wrinkling may arise in laminar or turbulent flow either side of the interface. The persistence of interface wrinkling and the repeated chopping-up and smoothing-out of sheared gas-liquid interfaces are more generally the visible phenomena of *interface-turbulence interactions*.

The concept of interface-turbulence interaction is relatively new and is of practical relevance in many applications. Liovic and Lakehal (2007a) showed the manner in which the turbulent energy cascade can be accompanied by an interfacial wrinkling cascade. It was shown in particular that small-wavelength wrinkling increases with *Re*, and is the result of vorticity outscatter in the gas-sided flow, to the extent that individual vortices nestled within individual interface wrinkles. The dampening of interface wrinkling has also been captured in the simulation of wave breaking by Liovic and Lakehal (2007b). Processes associated with the turbulent kinetic energy distribution play a major role in allowing surface smoothness to be regained, too. For instance back-scatter in the interface wrinkling cascade – which in the case of coastal wave breaking is characterized by the transition from 3D to 2D wrinkling – originates from the finest wrinkling scales through the action of surface tension.

Apart from turbulent flow, interface wrinkling is observed in small-scale flows in areas such as microfluidics and biomedical engineering. In biomedical engineering for instance, Ultrasound Contrast Agents (UCA) are microbubbles that clinicians seek to use for achieving sonoporation in the cerebral vasculature in order to facilitate drug delivery across the Blood-Brain Barrier (BBB) for the treatment of Alzheimer's Disease. Low sound-pressure excitation results in minimal deviation of microbubble shape away from sphericity, but the deviations away from it induced by sufficient sound pressure can be substantial. “Surface modes” in oscillating microbubbles (captured in photography by Dollet *et al*., 2008) are indeed higher-wavenumber interface wrinkles, and the modes included locally sharp gradients in curvature over the microbubble surface. In that essentially laminar forced-oscillating flow, the dissipative mechanism

of turbulence is not present and surface tension dominates at various stages during the oscillation.

The simulation methodology used by Liovic and Lakehal (2007a b) to capture interface-turbulence interactions is referred to as Large Eddy and Interface Simulation (LEIS). The core features of LEIS are: (i) the formalism of spatial scale separation achieved by scale high-pass filtering is borrowed from conventional LES of single-phase turbulent flows; (ii) interface tracking to infer resolved-scale interface dynamics; (iii) modelling the subgrid-scale (SGS) terms generated by filtering the microscale, multi-fluid flow equations. In comparison to LES of single-phase flow, LEIS involves more subgrid-scale (SGS) modelling effort, in that: (a) filtering is applied to microscale governing equations coupled at the interface via jump conditions; (b) filtering results in additional unclosed terms namely at the level of unresolved surface force; (c) SGS turbulence modelling requires additional (and relatively poorly understood) near-interface asymptotic behaviour to be captured and/or imposed, furthermore separately either side of the interfaces. Direct Numerical Simulation (DNS) of multi-fluid flow focuses on improving the accuracy of discretisation schemes with increasing mesh resolution. LEIS, on the other hand, primarily requires robustness in discretisation (albeit with lower-order schemes than DNS), as well as proper modelling support for the unresolved interfacial scales. The issue is whether these unresolved scales are tied to their turbulence counterparts - a question that is beyond the scope of this contribution.

In this paper, the LEIS methodology is presented, and the closure terms generated by filtering the transport equations are presented. The paper outlines in particular the first SGS model ever developed for unresolved surface tension. This work advances not only the ability of LEIS to simulate interface-turbulence interactions, but more generally presents an alternative approach to improved interfacial flow simulation that we consider to be more readily achievable elsewhere using generic multi-fluid flow solvers. In other words, the model is not meant for turbulent flows only, but should be applied in general to interfacial flows treated with interface tracking schemes.

## MODEL DESCRIPTION

### Continuum description

Volume tracking is applied to the single-field formalism for describing two-fluid flow by introducing a phase indicator function $C$

$$C(\mathbf{x}) = \begin{cases} 1 & \text{if } \mathbf{x} \text{ occupied by gas} \\ 0 & \text{if } \mathbf{x} \text{ occupied by liquid} \end{cases}. \quad (1)$$

In the continuous limit, $C$ is the Heaviside function. Tracking of the interface over time involves solving the topology equation

$$\frac{\partial C}{\partial t} + u \cdot \nabla C = 0 . \quad (2)$$

For isothermal incompressible flow conditions, volume conservation for individual fluid species aggregates into the Continuity Equation

$$\nabla \cdot u = 0 . \quad (3)$$

[For derivation of the single-field formalism from the multi-field description of multi-material flow featuring coupling through jump conditions, the interested reader is referred to Lakehal *et al.* (2002).]

In the continuum limit, conservation of momentum in the single-field formalism for interfacial flow is described by

$$\frac{\partial \rho u}{\partial t} + \nabla \cdot \left( \rho u u \right) = \nabla \cdot \prod + \rho \mathbf{g} + \sigma \kappa \hat{\mathbf{n}} \delta . \quad (4)$$

Equation (4) is similar in form to the momentum equations for single-phase flow, except now there is an extra term on the RHS describing surface tension that acts near the interface (as determined by $\delta$). The surface tension force is dependent on interface orientation and curvature: the former is a first-derivative of interface location

$$\hat{\mathbf{n}} = \frac{\nabla C}{\left| \nabla C \right|}, \quad (5)$$

while the latter requires the second-derivatives

$$\kappa = \nabla \cdot \hat{\mathbf{n}} . \quad (6)$$

### LEIS and filtered single-field formalism

The nonlinearity of the Navier-Stokes equations implies that any solution is dependent on even the smallest dynamic length scales in the flow. But since the smallest length scales cannot be systematically resolved by the grid, their coupling with the super-grid or resolved-scale solution needs to be modelled. Consistent with the LES concept, filtering the equations in this context applies in space only. More precisely, all dependent flow variables are decomposed into resolved- and subgrid-scale (SGS) components. When applied to the color function $C$ using

$$\overline{C}(\mathbf{x},t) \equiv G \otimes C = \int_D G(\mathbf{x} - \mathbf{x}') C(\mathbf{x}',t) \, d\mathbf{x}' \quad (7)$$

the filtered quantity is to be interpreted in this context as a resolved phase volume fraction. The interface is embedded in the spatial distribution $\overline{C}(x,y,z)$ as regions of $0 < \overline{C} < 1$. Of the many filters that are used in LES (refer to e.g. Sagaut, 2009), use is generally made of the tophat filter within the finite volume context.

Filtering of the color function equation yields

$$\frac{\partial \overline{C}}{\partial t} + \nabla \cdot \left( \overline{u} \overline{C} \right) = 0 . \quad (8)$$

In gas-liquid flows, discretisation of the single-field momentum equation (within the interface tracking framework) aims to achieve continuity of momentum by means of the jump conditions

$$\left[ \tau_N \right] = \left[ P \right] + \sigma \kappa , \quad (9)$$

$$\left[ \tau_S \right] = 0 . \quad (10)$$

Given filtering is applied on a term-by-term basis, care needs to be taken such that it preserves the fundamental properties of conservation, linearity and commutation with derivation (Sagaut, 2009), even in the interface regions. Therefore, one core feature of LEIS is the use of the density-based Component-Weighted Volume Averaging (CWVA) to complete the coupling (Lakehal, 2004):

$$f = \frac{\overline{\rho f}}{\overline{\rho}}, \quad (11)$$

which is analogous to Favre averaging for variable-density flow, and is readily extensible to compressible flow scenarios of interest (e.g. Ultrasound Contrast Agents). Applying CWVA to Equation (4) yields the filtered momentum equations (Liovic and Lakehal, 2007a b)

$$\frac{\partial \overline{\rho} \tilde{u}}{\partial t} + \nabla \cdot \left( \overline{\rho} \tilde{u} \tilde{u} \right) = + \nabla \cdot \left( \overline{\prod} - \tau^{SGS} \right) + \sigma \overline{\kappa} \overline{\hat{\mathbf{n}}} \delta , \quad (12)$$
$$+ \overline{\rho} \mathbf{g} + \varepsilon_C + \varepsilon_d + \varepsilon_\sigma$$

where $\varepsilon_k$ are the additional filtering-induced terms, which rigorously require closure. Of particular note is the fourth term

$$\varepsilon_\sigma = \sigma\overline{\kappa\hat{\mathbf{n}}\delta} - \sigma\overline{\kappa}\,\overline{\hat{\mathbf{n}}\delta}\,, \tag{13}$$

denoting the unresolved surface tension, and can in effect be non-negligible. The more familiar turbulence SGS stress term reads

$$\tau^{SGS} = \rho\left(\overline{uu} - \overline{u}\,\overline{u}\right). \tag{14}$$

[The addition of "interface" into the label LEIS refers to the fact that the "DNS of multi-fluid flow" is not achieved if terms such as those in Equations (13) and (14) are not negligible, especially if the observed convergence of a flow solver does not match that prescribed by its formal order of accuracy.]

#### Surface force modelling

The Continuum Surface Force (CSF) method (Brackbill *et al.*, 1992) is used with the delta function for near-interface proximity being approximated by the gradient in the color function, i.e.

$$\sigma\overline{\kappa\hat{\mathbf{n}}\delta} \approx \sigma\overline{\kappa}\nabla\overline{C}\,. \tag{15}$$

The gradient vector of $\overline{C}$ is determined by finite difference-based discretisation. The interface curvature $\overline{\kappa}$ is obtained from discretisation using the height function technique, in which heights are computed using

$$h_{i,j,k} = \sum_{kk} \overline{C}_{i,j,k+kk}\,\delta z_{k+kk} \tag{16}$$

and the curvature is subsequently computed as

$$\overline{\kappa} = \frac{h_{yy} + h_{zz} + h_{yy}h_z{}^2 + h_{zz}h_y{}^2 + 2h_{yz}h_yh_z}{\left(1 + h_y{}^2 + h_z{}^2\right)^{3/2}} \tag{17}$$

Details of height function-based curvature computation and the CSF methodology can be found in multiple sources (e.g. Liovic *et al*., 2009)).

#### SGS modelling on unresolved surface tension

*A priori* analysis of the turbulent flow around a rising gas bubble in liquid by Liovic and Lakehal (2007) showed the magnitude of the unresolved surface tension is unimportant relative to the turbulence counterpart (SGS stresses) in various regions of the flow. Cases of relatively poor interface resolution increase the effect of unresolved curvature contributions, while flow relaminarization reduces the magnitude of the SGS stresses.

The need for closure of the unresolved surface tension term in Equation (13) has been recognized as important for interfacial flow simulation in various studies, yet little progress in achieving verified, practical closure for it has been made thus far. Herrmann and Gorokhovski (2008) proposed explicit filtering based on knowledge of "exact" curvatures and normals. Their approach remains untested, and the need for a refined level-set method to represent the exact interface limits its scope. Alajbegovic (2001) also proposed a form of a model for unresolved curvature, though linking it to the SGS turbulence scales. The justification for this linkage is not obvious, given the curvature (resolved or SGS) is specifically a property of interface topology (i.e. it could happen for laminar interfacial flows as well). Again, the proposed model was not accompanied by any testing.

We propose in this work a rather surface topology-based alternative modelling approach, that is all the more functional and easily implemented and is verified as being effective in capturing unresolved surface tension.

In LEIS, dependent variables are implicitly filtered by the process of spatial discretisation – equivalent to a tophat filter matching the mesh spacing. Wider filters can also be applied to discretisation scheme outputs, and inputs into discretisation schemes may also be coarse-filtered variables. These distinctions are important for formulating an SGS surface force model. We first proceed by distinguishing between a 2Δ-filtered curvature based on direct filtering of the super-grid curvature, and a 2Δ-filtered curvature based on discretisation using a 2Δ-filtered interface representation. The former is denoted as

$$\overline{\boldsymbol{\kappa}}^{2\Delta\left[\kappa(\delta x)\right]}, \tag{18}$$

with the bar on the curvature preserved to indicate it is computed using explicit convolution (Equation (7)), where the filtering uses discretisation-based curvature estimates from the regular mesh an input. The latter is denoted as

$$\boldsymbol{\kappa}^{\Delta\left[\overline{C}(2\Delta)\right]}, \tag{19}$$

with the bar on the curvature dropped to indicate it is computed using the discretisation formula (Equation (17)) and using explicitly coarse-filtered color function data as an input. This is equivalent to computing curvature using Equation (17) and height function data on a twice-as-wide stencil. Similar is also done to generate 3Δ-filtered curvature estimates: the first is based on direct filtering $\overline{\boldsymbol{\kappa}}^{3\Delta\left[\kappa(\delta x)\right]}$ and the second is based on discretisation $\boldsymbol{\kappa}^{\Delta\left[\overline{C}(3\Delta)\right]}$, respectively.

The coarse-grid-data curvature constructs are the basis of the SGS surface tension model procedure. In this, the differences between filtered curvature estimates generated by direct filtering and discretisation are used to identify the presence of unresolved contributions to the unfiltered curvature; we denote the unresolved curvature as $\boldsymbol{\kappa}^{SGS}$.

Analysis of variations in curvature estimates enables SGS modes to be detected, which is readily possible because low-order height function-based curvature discretisation filters out SGS curvature modes. For example, consider the case of the regular-mesh curvature estimate $\boldsymbol{\kappa}^{\Delta(\overline{C}(\Delta))}$ being smaller than the coarse-filtered-$C$ discretized curvature $\boldsymbol{\kappa}^{\Delta(\overline{C}(2\Delta))}$. Intuition suggests us to infer that the bulk of the contribution to the magnitude $\boldsymbol{\kappa}^{\Delta(\overline{C}(2\Delta))}$ appears from the parts of the wider stencil not overlapped by the regular stencil. Based on that reasoning, one can expect the centre of the stencil to be a relatively low-curvature zone - the curvature at the centre of the stencil in the limit of $\delta x \to 0$ is presumed to be smaller than that computed from regular discretisation, making $\boldsymbol{\kappa}^{SGS}$ negative. Similarly, $\boldsymbol{\kappa}^{\Delta(\overline{C}(\Delta))}$ being larger than $\boldsymbol{\kappa}^{\Delta(\overline{C}(2\Delta))}$ indicates that the unfiltered curvature is larger than that predicted by discretisation, therefore inviting a positive $\boldsymbol{\kappa}^{SGS}$ contribution to add subgrid-scale interface wrinkling to compensate for small interfacial length-scale detail that discretisation cannot capture.

Curvature estimates obtained from direct filtering using coarser filters are used to prove consistency of curvature variation across the breadth of discretisation stencils. Consistency in the trends of curvature change with filter width help confirm that an estimate of $\boldsymbol{\kappa}^{SGS}$ is geometrically sensible: if the curvature changes are not

consistent, then the regular-mesh curvature estimate cannot be assumed to be sensible. In such cases, the pool of coarse-discretisation and coarse-filter curvature estimates can also be used to override regular-mesh estimates by imposing more geometrically realistic estimates, thereby making $\kappa^{SGS}$ locally more substantial.

Drawing analogy with established methods for SGS modelling in LES of turbulent flow, the procedure presented here combines ideas underpinning various modelling approaches. In the case of directly filtered curvatures verifying discretisation-based curvature variations with changing filter width, the magnitude of the prescribed SGS curvature varies consistently with the difference between filtered estimates – proportionality on a derived quantity that makes the SGS curvature procedure resemble Smagorinsky-kernel models in LES. When the pool of filtered curvature estimates are found to be inconsistent, replacing the regular discretisation curvature estimate with a "curvature-limited" value gives the SGS curvature procedure a sensibly physics-based property – similar to the action of flux-limiting in momentum advection schemes in Monotone-Integrated Large Eddy Simulation (MILES) of Boris (1990). The methodology indeed imposes a physically sound energy transfer between length scales in the vicinity of the filter scales. More details on the new SGS curvature procedure are included in Liovic (2009).

### SGS stress closure

The established LES methodology is rich with modelling approaches for the SGS stress tensor, such as effective eddy-viscosity models, scale similarity models and deconvolution models, among many others. [The readers are referred to Sagaut (2009) for an overview.] Despite the abundance of SGS modelling approach, a common drawback is their inability to properly capture the turbulence asymptotic behaviour approaching solid surfaces, and also near arbitrarily-deformable gas-liquid interfaces. The state-of-the-art for LEIS involves indeed correcting the physics of near-interface turbulence decay, as inspired by Lakehal and coworkers (Reboux *et al*., 2006; Liovic and Lakehal, 2007). "Interface asymptotic behaviour" is imposed upon an underlying SGS model in the form of a damping function equivalent to the van Driest damping function for wall flows. The methods can be incorporated into VOF-based interface tracking solvers using the Reconstructed Interfacial Shear Velocity (RISV) algorithm (Liovic and Lakehal, 2007b), or directly using Level-Set techniques (TransAT, 2009).

## NUMERICAL EXPERIMENTS

### 3D cosine wave

The 3D cosine wave test (Liovic *et al*., 2009) is a more challenging test of curvature schemes than the well-documented sphere test, because the curvature distribution is not spatially uniform and changes relative to mesh size. For any (*x*,*y*) coordinate, the cosine wave is initialized as

$$z_{wave} = A - B\cos\left(\frac{2n\pi w}{L}\right) \qquad (20)$$

where $w$ is the projection of the 2D coordinate vector $x\mathbf{i} + y\mathbf{j}$ onto the propagation direction $\mathbf{p} = \mathbf{i} + \mathbf{j}$. In the current test, we use $L = 8$, $A = 4$, $B = 1$ and $n = 4$; the resultant interface shape is shown in Figure 1. The exact curvature corresponding to a 2D cosine wave propagated in the direction of increasing $w$ is

$$\kappa_{exact} = -\frac{z''}{\left(1 + (z')^2\right)^{3/2}}. \qquad (21)$$

The wave features high-curvature peaks and troughs that curvature discretisations are known to have difficulty resolving, and for which SGS modelling support is particularly desirable. The setup has low-curvature regions as well, such that discretisation should adequately resolve, and for which SGS closure should be negligible.

In the current test, the regular-mesh discretisation-based curvature estimate is computed using the height function scheme. In the SGS curvature procedure, the same height function-based curvature scheme is then used with wider-stencil inputs for discretisation-based filtered curvature estimates (along with direct filtering estimates). The performance of the SGS curvature modelling is assessed by comparing the $L_1$ errors of the procedure to those based on regular discretisation:

$$L_1 = \sum \left|\nabla C\right|_{i,j,k} \left|\overline{\kappa}_{i,j,k} - \kappa_{exact}\right| \delta V_{i,j,k}. \qquad (22)$$

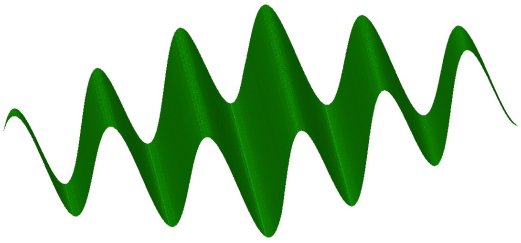

**Figure 1**: Initialization of interface shape for 3D cosine wave problem.

Table 1 shows the $L_1$ errors obtained for curvature estimation with and without SGS curvature modelling support. It shows that 20-to-30 percent reductions in curvature error can be achieved using the model, and this figure should be improved on with more work. The most noteworthy part of the outcome is that the test problem is difficult and includes under-resolved areas and locally high curvatures and high-wavenumber interface wrinkling. The results show that the modelling procedure is capable of detecting that wrinkling, and to some extent compensating for the under-resolution of discretisation.

| Grid | Discretisation | Discretisation+SGS |
|---|---|---|
| 32×32×32 | $1.77\times10^{-4}$ | $1.40\times10^{-4}$ |
| 64×64×64 | $1.61\times10^{-4}$ | $1.18\times10^{-4}$ |

**Table 1**: Comparison of $L_1$ error in curvature for 3D cosine wave problem, from height function-based discretisation alone, and from discretisation plus SGS curvature contributions predicted by the procedure.

### 3D bubble bursting at a free surface

The bursting of a bubble at a free surface is an important problem in nature, and in conventional and novel technologies. Sea spray drops ejected by bursting bubbles in oceans are important for fog and cloud formation. In pyrometallurgical smelters, splash drops are important for

the downward transport of heat from post-combustion in the freeboard space into the bath.

Experimental investigations of a single bubble bursting at a free surface date back to Kientzler *et al.* (1954). Examples of simulation include the boundary-integral method (Boulton-Stone and Blake, 1993), and multi-material DNS using markers for interface tracking (Duchemin *et al.*, 2002). We note that the numerical studies used problem initializations that feature just-burst bubbles and seek to simulate jet formation and any drops that tear off from the jet. In reality, the phenomenon observed in experiment is more detailed than the simulation setups considered in these past investigations. Günther *et al*. (2003) summarize the distinction between drops formed from jet break-up, and drops formed previously to that by film rupture. In bypassing film drainage and rupture, computational studies conducted hitherto decouple bubble rise from bubble bursting.

Bubble rise and splash drop generation as decoupled events have been simulated and validated extensively by the MFVOF code. Documented examples include single and multiple bubble formation and rise, and splash generated by an impinging drop. The codes have also simulated coupled bubbling and splashing in the same computation, in the context of continuously sparged vessels. [Further details in Liovic *et al.* (2007a b) and earlier references.] In the coupled-bubbling/splashing simulations, filter-scale physics and phenomenology are coarse-grained. The current work represents an attempt to reduce the coarse-graining associated with film rupture and transition in dispersed phase from gas to liquid.

A first example of the bubble bursting event coupling bubble rise, film rupture and droplet generation is demonstrated in Figure 2. In the simulated setup, a 10mm diameter air bubble rising through a highly viscous liquid ($\mu_L > 10^{-1} Pa.s$) disengages at a free surface. As a first simulation attempt, the setup does not conform for now to a specific experiment. In this case, ramping up of the liquid viscosity in this problem results in retarded liquid film drainage, hence results in the bubble cap protruding above quiescent free-surface level and a film of non-negligible curvature, as shown in Figure 2(a). The significant protrusion of the draining film above the quiescent free surface level results in a film liquid volume for film rupture and break-up (shown in Figure 2(b)) that would be larger than for a similar bubble size in water. Post-processing of Figure 2(c) yields 358 drops, of which 201 constitute sub-filter scales, where the filter-scale is $\Delta = 350 \mu m$. Typical numbers from experiment for the number of film droplets generated by film rupture in the bubble bursting event are $O(10^2)$; for the air-water system, results summarized by Günther *et al*. (2003) predict that about 100 droplets should be generated from the film liquid (on a time scale ahead of jet break-up).

The droplets generated by film break-up are ejected well above the free surface, as shown in Figure 3. The number of droplets involved and the velocities result in turbulence generation in the gas-sided flow. In contrast to single-phase turbulent flows, in interfacial flows, turbulence is indeed bubble- or droplet-based, rather than only shear-based. Small-scale structures (length and velocity scales) depend on the population balance of the inclusions (droplets or bubbles).

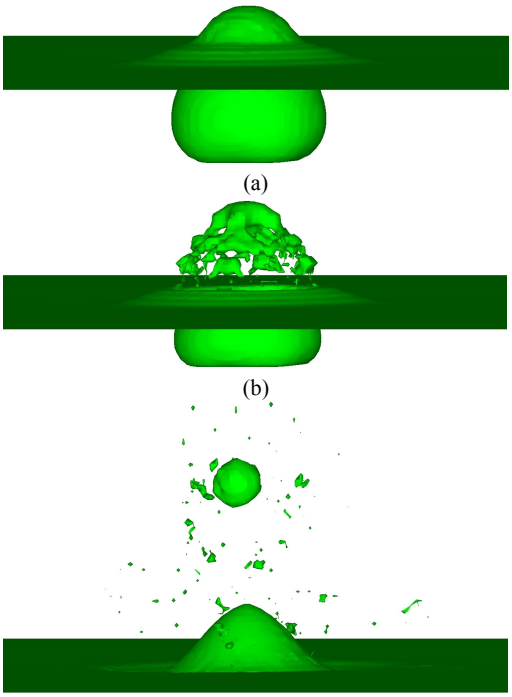


**Figure 2**: Bubble bursting at a free surface, simulated in 3D: (a) rise of bubble through free surface level initiates film drainage; (b) 3D film break-up; (c) multiple splash droplets due to film breakup.

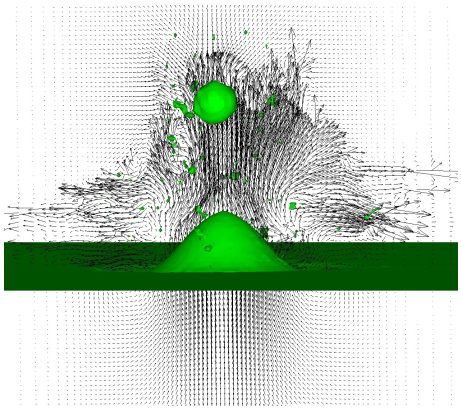

**Figure 3**: Velocity field in 2D slice through geometric centre of flow, showing turbulence generation above the free surface in the aftermath of bubble bursting.

A 2D slice through the geometric centre of the bubble is shown in Figure 4. The lower regions of the bubble, the top and the free surface centrally above it have relatively smooth small-multiple spatial variations in curvature away from that corresponding to the equivalent-volume sphere. In the azimuth corresponding to minimum film thickness in Figure 4(a), the free surface and the bubble surface bounding the film feature maximum curvature in the flow domain. The high curvature is primarily a result of azimuthal modes in the film break-up, as seen in Figure 2(b) – an illustrative example of surface tension-induced flow instability initiating 3D interface wrinkling even in non-turbulent flows, as explained in the Introduction.

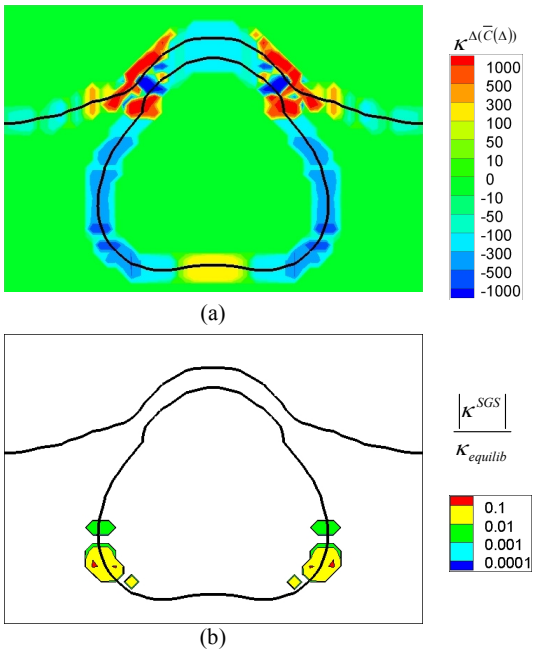


**Figure 4**: (a) Unfiltered and (b) SGS curvature at the free surface and bubble interface in the early stages of film drainage prior to bubble bursting. The magnitude of the SGS curvature is scaled by $\kappa_{equilib} = 400$ .

The SGS curvature model applied to a topology snapshot yields the distribution shown in Figure 4(b). The procedure yields non-zero $\kappa^{SGS}$ in localized regions of the lower bubble surface, of magnitudes as high as 10 percent of the actual curvature. These numbers and levels are sufficient to affect surface tension-induced instabilities, in particular in small-scale interfacial flows (e.g. microfluidics). [These magnitudes were also commonly seen in the 3D cosine wave test.] The film region and the multitude of SGS fluid filaments created during film break-up present major challenges to curvature discretisation and subsequent curvature filtering operations. As designed thus far for stability, the SGS curvature model does not add contributions indiscriminately; non-zero $\kappa^{SGS}$ is only accounted for when the decision mechanism between the multi-scale discretized and directly-filtered curvature estimates unambiguously prescribes it. Evolving the SGS curvature procedure to prescribe realistic SGS curvature in the case of SGS fluid filaments represents future work; such work may also require consideration of $\varepsilon_d$ .

## CONCLUSION

The Large Eddy and Interface Simulation (LEIS) for 3D interfacial dynamics investigation has been enhanced with the modelling of unresolved surface tension, which is meant for both laminar and turbulent flows. Beyond the usual surface tension discretisation schemes proposed in the literature, the unresolved surface tension model is capable of prescribing additional or less curvature where the local analysis of the interface geometry requires it. The SGS surface tension modelling procedure helps promote the high-fidelity capturing of fine-scale interface wrinkling in a stable interfacial flow simulation context using moderate computing resources.


## ACKNOWLEDGEMENTS

This work was supported by the NCI National Facility at the Australian National University.


## REFERENCES


ALAJBEGOVIC, A., (2001), "Large Eddy Simulation formalism applied to multiphase flows", *Proc. ASME Fluids Eng. Div. Summer Meeting*, New Orleans, 29 May-1 June, FEDSM2001-18192.

BORIS, J.P., (1990), "On large eddy simulation using subgrid turbulence models", *Whither Turbulence? Turbulence at the Crossroads*, (Ed. J.L. Lumley), 344-353, Springer-Verlag.

BOULTON-STONE, J.M., BLAKE, J.R., (1993), "Gas bubbles bursting at a free surface", *J. Fluid Mech.*, **254**, 437-466.

BRACKBILL, J.U., ZEMACH, C., KOTHE, D.B., (1992), "A continuum method for modeling surface tension", *J. Comput. Phys.*, **100**, 335-354.

DUCHEMIN, L., POPINET, S., JOSSERAND, J., ZALESKI, S., (2002), "Jet formation in bubbles bursting at a free surface", *Phys. Fluids*, **14**, 3000-3008.

DOLLET, B., VAN DER MEER, S.M., GARBIN, V., DE JONG, N., LOHSE, D., VERSLUIS, M., (2008), "Nonspherical oscillations of ultrasound contrast agent microbubbles", *Ultrasound in Medicine and Biology*, **34**, 1465-1473.

GÜNTHER, A., WÄLCHLI, S., RUDOLF VON ROHR, P., (2003), "Droplet production from disintegrating bubbles at water surfaces. Single vs multiple bubbles", *Int. J. Multiphase Flow*, **29**, 795-811.

HERRMANN, M., GOROKHOVSKI, M., (2008), "An outline of an LES subgrid model for liquid/gas phase interface dynamics", *Proc. Summer Program – Center for Turbulence Research*, Stanford.

KIENTZLER, C.F., ARONS, A.B., BLANCHARD, D.C., WOODCOCK, A.H., (1954), "Photographic investigation of the projection of droplets by bubbles bursting at a water surface", *Tellus,* **6**, 1-7.

LAKEHAL, D., (2004), "DNS and LES of turbulent multifluid flows", Keynote. *Third Int. Symp. Two-Phase Flow Modelling and Experimentation*, Pisa, 22-24 September.

LAKEHAL, D., MEIER, M., FULGOSI, M., (2002), "Interface tracking for the prediction of interfacial dynamics and heat/mass transfer in multiphase flows", *Int. J.Heat Fluid Flow*, **23**, 242-257.

LIOVIC, P., LAKEHAL, D., (2007a), "Interface-turbulence interactions in large-scale bubbling processes", Int. *J.Heat Fluid Flow*, **28**, 127-144.

LIOVIC, P., LAKEHAL, D., (2007b), "Multi-physics treatment in the vicinity of arbitrarily deformable gas-liquid interfaces", *J. Comput. Phys.*, **222**, 504-535.

LIOVIC, P., (2009), "Towards closure of subgrid-scale surface tension in interfacial flow simulation", *Comp. Fluids*, (in review).

REBOUX, S., SAGAUT, P., LAKEHAL, D., (2006), "Large Eddy Simulation of sheared interfacial two-fluid flow using the Variational Multiscale Approach", *Phys. Fluids*, **18**, 105105-1-15.

SAGAUT, P., (2009), *Large Eddy Simulation for incompressible flows*, Springer.

TRANSAT., (2009), TransAT: Transport Phenomena Analysis Tool, *ASCOMP GmbH, Zürich, Switzerland*, www.ascomp.ch/transat.html.